

## Propagation Properties of Multilayer Thin-Film Polarization-Maintaining Optical 3-D Waveguide

Hsu, Jui-Pang Tetsuo Anada Sadaoki Nakamura Tunchisa Kobayashi

Faculty of Engineering, KANAGAWA UNIVERSITY  
221, Yokohama Japan

**Abstract-** We propose a new single-mode and polarization-maintaining three-dimensional optical waveguide. The structure of the optical waveguide proposed here consists of lamination of very thin-films of two optical materials with different refractive indices and the rib-type waveguide for the confinement of the optical field in the vertical and horizontal direction respectively. The method of analysis is fundamentally based on the equivalent multi-mode transmission line model and the transverse resonance condition. By this method, the propagation properties of the guided wave for various structure parameters are investigated. Some new numerical and useful results are obtained.

### I. Introduction

A single-mode and polarization-maintaining planar-type three dimensional(3-D) optical waveguide will be strongly needed in near future for the integration of optical circuits.

This need will be accelerated with the advent of a single-mode and polarization-maintaining optical fiber. The conventional three or four layers or ion-exchanged optical waveguides have two types of propagation modes, i.e. TE-like and TM-like modes. However they are almost degenerate for any case so that it is difficult to realize the single-mode and polarization-maintaining optical waveguide with these structure. On the other hand, it is well-known that the lamination of very thin-films of two optical materials with different refractive indices exhibits the artificial birefringence effect[1]-[4]. Basing upon these properties, we propose a new planar-type 3-D optical waveguide. Thus the structure consists of the lamination of very thin-films of two different optical materials and of rib-type side structure, as shown in Fig.1.

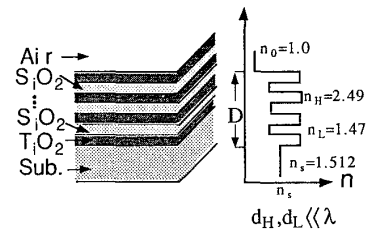
As for the method of analysis, many numerical or analytical methods have been developed to study the propagation characteristics of 3-D optical waveguides. However, surface-wave planar circuit concept[6] is used here. The method is fundamentally based on the equivalent multi-mode transmission lines model in the vertical and horizontal direction and the transverse resonance conditions.

Finally practical 3-D multilayered optical waveguides, which consists of the lamination of SiO<sub>2</sub> and TiO<sub>2</sub> on the substrate as shown in Fig.1, are analyzed and numerically discussed. Some useful results are obtained.

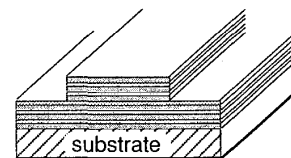
### II. Structure and Method of Analysis

#### A. Structure and Working Mechanism

The structure of the 3-D optical waveguide proposed here consists of the lamination of very thin-films of two different optical materials and of rib-type side structure for the confinement of the optical field in the vertical and horizontal direction respectively. The former structure is used for the realization of large separation of TE and TM mode degenerate situation, where optical materials of the film( $n_L$  and  $n_H$ ) and substrate( $n_s$ ) combination of these optical material, the ratio( $R=d_H/d_L$ )



(a) Multilayered thin-film slab structure and refractive index distribution.



(b) Rib type 3-D optical waveguide

Fig.1 Structure of the multilayered thin-film three dimensional optical waveguide.

of the thickness of the two laminated optical material, number of thin-film layers( $N$ ), total thickness( $D$ ) and operating wavelength( $\lambda$ ) will contribute to the value of effective refractive index of the dominant mode and the degree of mode separation which, in return, can be used for the control of mode separation degree and effective refractive index of the dominant mode; the latter structure is used for the mode suppression of the unwanted higher modes, where the parameter of rib-type side structure(i.e. total thickness( $D'$ ) and number of thin-film layers( $N'$ ) will contribute to vary the effective refractive index which, in return, can be used for the control of the unwanted higher modes radiation[5]. Through these mechanism, the single-mode and polarization-maintaining 3-D optical waveguide is realized.

#### B. Method of analysis

Since the theoretical treatment has been described by the authors[6]-[7], only the principle steps will be explained.

The method is fundamentally based on the equivalent multi-mode transmission line model in the vertical and horizontal direction and the transverse resonance condition. The corresponding equivalent transmission line model in two direction are derived from the surface-wave planar circuit[6] and mode coupling equations at step discontinuity[7] as shown in Fig.2.

Based on these equivalent circuit and definition of mode voltage column matrix at port 1 and port 2, the following characteristic matrix equation is obtained.

$$\begin{pmatrix} -Y_{c\perp} \cot(\beta_{\perp} W) + Y_W^{(1)} & jY_{c\perp} \operatorname{cosec}(\beta_{\perp} W) \\ jY_{c\perp} \operatorname{cosec}(\beta_{\perp} W) & -Y_{c\perp} \cot(\beta_{\perp} W) + Y_W^{(2)} \end{pmatrix} \begin{pmatrix} V^{(1)} \\ V^{(2)} \end{pmatrix} = 0$$

where  $Y_W^{(1)}, Y_W^{(2)}$  are effective side-wall admittance.

$$Y_W^{(1)} = Y_W^{(2)} = \begin{pmatrix} Y_{\text{eff}}^{1H1H} & Y_{\text{eff}}^{1H1E} \\ Y_{\text{eff}}^{1E1H} & Y_{\text{eff}}^{1E1E} \end{pmatrix}$$

By making the determinant of this matrices zero, propagation constants of the 3-D optical waveguide can be calculated. Also from the eigenvector, the transverse field distribution of the propagation modes can be calculated.

Hence, the first step in the analysis is to find the propagation constants and eigenfunctions of waves propagating in the multilayered thin-film slab structure of inside and outside from table I. This step makes it possible to express the transverse components of the electromagnetic fields in inside and outside. The next step is to look the mode voltage and current amplitudes which satisfy the continuity conditions of the tangential fields at the rib-type step discontinuity by using above mentioned matrix equations.

In these analysis, sufficient number of each TE and TM mode are taken into consideration in order to satisfy the continuity condition of the tangential field components at the step discontinuity in rib-type waveguide.

Also non-radiative continuous spectrum is discretized by placing the metallic top and bottom walls properly and far away from the optical waveguide.

### III. Numerical Results

The propagation constants and the corresponding field distributions for the practical structure shown in Fig.1 are calculated, based on the above mentioned method. The structure parameters are chosen as follows: refractive index of  $TiO_2$ :  $n_H=2.49$ ,  $SiO_2$ :  $n_L=1.47$ , substrate:  $n_S=1.512$ , the ratio of thin-film layer  $d_H/d_L=0.2$ , the total thin-film thickness  $D=0.6\mu m$ , and the operating wavelength  $\lambda=0.6328\mu m$  is assumed.

Here also following items are investigated.

1. necessary number of thin-film layers to separate TE and TM propagation modes sufficiently.
2. necessary number of thin-film layers at the rib-type side structure to realize a single mode and polarization-maintaining character.
3. necessary number of TE and TM higher modes to describe the transverse field distribution of optical waveguide fully.

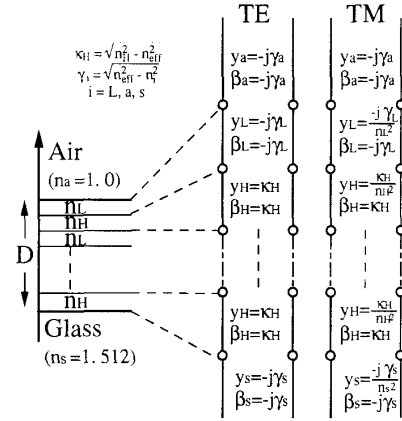
#### A. Effective refractive index for the multilayered thin-film slab

Usually it is pointed out that when  $d_H, d_L \ll \lambda$ , large birefringence effects appear, but it is not clear how much small to make the dimensions of  $d_H$  and  $d_L$ . In order to investigate how many layers are necessary to separate TE and TM mode, the effective refractive index for multilayered slab structure with a given total thickness are calculated as a function of the number of layers and the ratio  $R=d_H/d_L$ . One of the numerical results with  $R=0.2$ ,  $D=0.6\mu m$  is shown in Fig.3. From Fig.3, we can say that the effective refractive index for each mode will converge to a certain value with the number of layers; it is almost converged beyond  $N=10$  layers. Hence, in the following calculation 10 layers with  $D=0.6\mu m$  are assumed at the inside guiding structure.

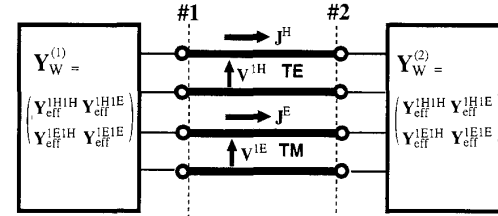
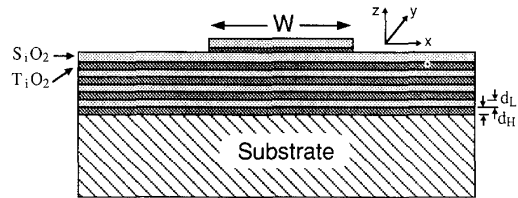
#### B. Propagation constants of 3-D rib-type optical waveguide

Propagation constants of the practical rib-type 3-D optical waveguide are calculated as a function of waveguide width  $W$  with the number of rib-type side layers as a parameter.

The calculated results are shown in Figs.4, where the results of step-type side structure are also shown in Fig.4(a) for the



(a) Transmission line model in the height direction



(b) Transmission line model in the horizontal direction

Fig.2 Multilayered thin-film rib-type 3-D waveguide and its equivalent circuit .

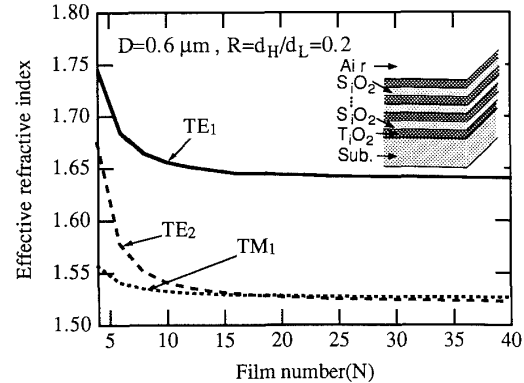


Fig.3 Effective refractive index of  $TE_1, TE_2, TM_1$  as a function of the number of thin-film layer

comparison and discussion. From these figure we can say that  
 1) There exist 2 TE and 1 TM surface-modes in the main structure as clear from Fig.3.

2) For the step-side structure, all 3 surface-modes are totally reflected at the both sides so that there exist three kinds of TE-like and TM-like modes.

3) When 4 layers of rib-type side structure, the effective refractive index of the side structure becomes  $n_{\text{eff}}=1.56$ , which makes the TM<sub>1</sub>, and TE<sub>2</sub> surface-modes of the inside structure to radiate outside. Hence only TE<sub>1</sub> mode exists below  $W=1\mu\text{m}$  width: the optical waveguide can be operated as the single mode and TE-polarization maintaining waveguide.

4) As number of layers at the side structure are increased more, the waveguide operates as a single mode and TE-polarized mode in the range up to line-width  $W=2.0\mu\text{m}$ . For example, the range is increased from  $1\mu\text{m}$  (4-layers in Fig.4(b)) to about  $2\mu\text{m}$  (8-layers in Fig.4(d)).

### C. Field distribution of the 3-D optical waveguide

At the rib-type step discontinuity, higher TE and TM modes are excited to satisfy the boundary conditions. Enough number of higher TE and TM modes then are taken into account according to the accuracy required. In this case, 25 TE and 25 TM modes are taken at each region. As an example, Figs.5 show the field distributions over cross section for the dominant TE-like mode ( $E_{11}^X$ ) and second higher width TE-like mode ( $E_{21}^X$ ) at the points labeled on curves in Fig.4(a), (d).

## IV. Conclusion

A new single-mode and polarization-maintaining 3-D rib-type optical waveguide having the multilayered thin-film structure is proposed, and its propagation properties are analyzed based on the surface-wave planar concept.

Following conclusions are also obtained for the multilayered thin-films of  $T_1O_2$  and  $S_1O_2$  materials.

1. About  $N=10$  layers are enough to separate TE and TM mode sufficiently.
2. Ratio of  $dH/dL=0.2$  gives the reasonable effective refractive index for the dominant mode.
3. Number of thin-film layer at the rib-type side structure can surely control the unwanted higher modes to radiate.
4. 25 TE and 25 TM modes are roughly enough to describe the two dimensional field distribution of the 3-D optical waveguide.

## Reference

- (1) M. Born and E. Wolf, "Principles of Optics", MacMillan, New York, 1964.
- (2) J.P. van der Ziel, M. Ilegerns and R. M. Mikulyak, "Optical birefringence of thin GaAs-AlAs multilayer films", Appl. Phys. Lett., vol.28, No. 12, pp.735-737, 15 June, 1976.
- (3) M. Kitagawa and M. Tateda, "Form birefringence of  $S_1O_2/Ta_2O_5$  periodic multilayers", Appl. Opt., vol. 24, No. 20, pp.3359-3362, 15 Oct., 1985.
- (4) Y. Fujii, "Anomalous Birefringence in Very Thin Layered Structure", IEICE Japan Tech. Rep., OQE85-156, pp.1-6
- (5) S. T. Peng and A. A. Oliner, "Guidance and Leakage properties of a class of open dielectric waveguides: Part I - Mathematical formulations," IEEE Trans. MTT., vol. MTT-29, pp. 843-854, 1981.
- (6) Hsu, Jui-Pang, T. Anada, F. Eriguchi, "Proposal on surface-wave planar circuit, Formulation of its planar circuit equations and its practical application", 1986 IEEE MTT-S Digest., GG-4, pp.797-800.
- (7) Hsu, Jui-Pang, T. Anada, A. A. Oliner, S. T. Peng, "Formulation of mode coupling equations at step discontinuity based on the planar circuit theory", 1989 IEEE MTT-S Digest., pp-5, pp.1135-1138.

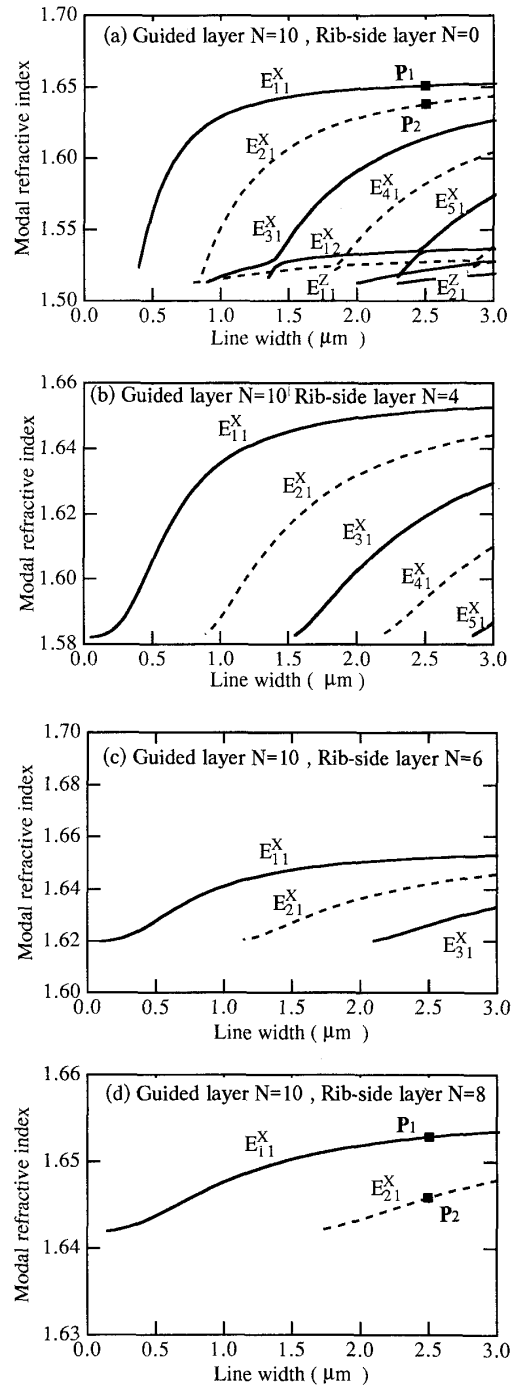


Fig.4 Modal refractive index plotted as a function of the line-width for multilayered thin-film polarization-maintaining 3-D optical waveguide.

Table I Fundamental relation of surface-wave planar circuit

	TE (H) MODE	TM (E) MODE
Field component	$H_z(x,y,z) \equiv -\sum_n V_n^H(x,y) \cdot g_n^H(z)$ $\mathbf{E}_t(x,y,z) \equiv \sum_n [\mathbf{J}_n^H(x,y) \times \mathbf{k}] \cdot f_n^H(z)$ $\mathbf{H}_t(x,y,z) \equiv (j\eta_0)^{-1} \sum_n \mathbf{J}_n^H(x,y) \cdot h_n^H(z)$	$H_z(x,y,z) \equiv -\sum_n V_n^E(x,y) \cdot g_n^E(z)$ $\mathbf{E}_t(x,y,z) \equiv \sum_n [\mathbf{k} \times \mathbf{J}_n^E(x,y)] \cdot f_n^E(z)$ $\mathbf{H}_t(x,y,z) \equiv j\eta_0 \sum_n \mathbf{J}_n^E(x,y) \cdot h_n^E(z)$
Basic surface-wave	$\frac{d^2 g_n^H}{dz^2} + [k_0^2 \epsilon_s(z) - (\beta_n^H)^2] g_n^H = 0$ $f_n^H = g_n^H, \quad h_n^H = \frac{1}{k_0} \frac{df_n^H}{dz}$ $\langle g_m^H, f_n^H \rangle = \int g_m^H f_n^H dz = \delta_{mn}$	$\frac{d}{dz} \left[ \frac{1}{\epsilon_s(z)} \frac{d}{dz} (\epsilon_s(z) g_n^E) \right] + [k_0^2 \epsilon_s(z) - (\beta_n^E)^2] g_n^E = 0$ $f_n^E = g_n^E, \quad h_n^E = \frac{1}{k_0} \frac{1}{\omega \epsilon_0} \frac{df_n^E}{dz}$ $\langle g_m^E, f_n^E \rangle = \int g_m^E f_n^E dz = \delta_{mn}$

$\mathbf{k}$ : unit vector toward height direction

$$V(x,y) = (Ae^{-j\beta_L x} + Be^{j\beta_L x}) e^{-j\beta_T y}$$

$$Y_{CL} = Y_C (\beta_L / \beta_T) \quad Y_{CT} = Y_C (\beta_T / \beta_L)$$

$$\beta_L = \sqrt{\beta_T^2 - \beta_z^2} \quad \beta_T = \beta_n$$

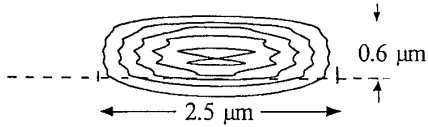
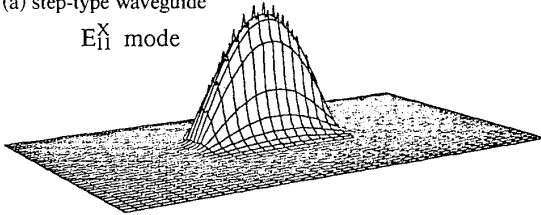
$$k_0 = \omega_0 / \epsilon_0 \mu \quad \eta_0 = \sqrt{\mu / \epsilon_0}$$

$$J_{\perp}(x,y) = Y_{CL} (Ae^{-j\beta_L x} - Be^{j\beta_L x}) e^{-j\beta_T y}$$

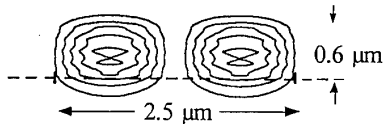
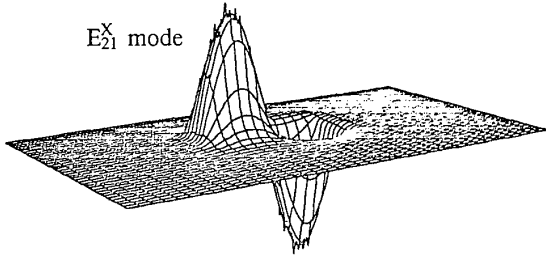
$$J_{\parallel}(x,y) = Y_{CT} (Ae^{-j\beta_L x} + Be^{j\beta_L x}) e^{-j\beta_T y}$$

(a) step-type waveguide

$E_{11}^X$  mode

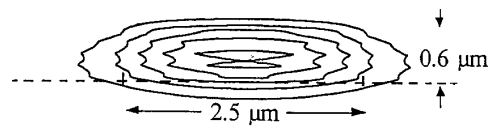
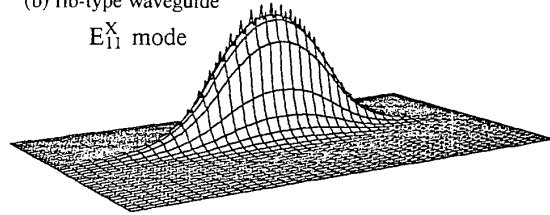


$E_{21}^X$  mode



(b) rib-type waveguide

$E_{11}^X$  mode



$E_{21}^X$  mode

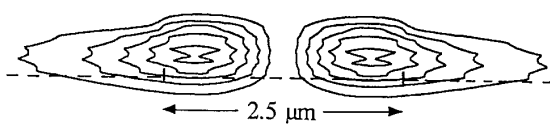
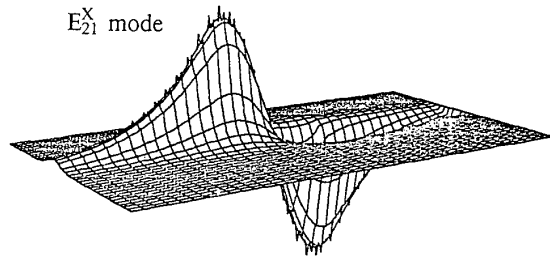


Fig.5 Field distributions of the dominant  $E_{11}^X$  and second higher  $E_{21}^X$  mode at the points labeled on curves in Figs.4(a), (d). (a) step-type waveguide in Fig.4(a); (b) rib-type waveguide in Fig.4(d).